Polymer Networks

DOI: 10.1002/anie.200705079

Surface Synthesis of 2D Branched Polymer Nanostructures

Sigrid Weigelt, Carsten Busse, Christian Bombis, Martin M. Knudsen, Kurt V. Gothelf, Erik Lægsgaard, Flemming Besenbacher, and Trolle R. Linderoth**

Molecular nanostructures formed by bottom-up self-organization[1] are model systems for advanced functional surfaces with a broad range of applications, such as sensors or coatings, molecular electronics, and heterogeneous catalysis. Supramolecular structures formed on surfaces under ultrahigh-vacuum (UHV) conditions through exploitation of noncovalent interactions, such as van der Waals forces,[2] dipole–dipole interactions,[3] hydrogen bonding,[4] or metal complexation,[5] have been studied extensively with scanning tunneling microscopy (STM). Structures stabilized by stronger covalent bonds between the molecular building blocks are anticipated to have an improved thermal and chemical stability, and are thus likely to be more useful for practical applications. However, investigations into covalently interlinked molecular structures on surfaces under UHV conditions are only just emerging.[6]

Thin films produced by vapor-deposition polymerization[7] have been studied by STM, as has photoinduced or STM-tip-induced polymerization of diacetylene.[8] Macromolecules have been deposited at surfaces using the pulse injection technique[9,10] and characterized at modest resolution, and polymer architecture and folding have been studied upon electropolymerization[11] or drop-casting.[12] Although polymers deposited or formed in UHV[6,8,13] and at the liquid/solid interface[11,12] have been observed, no detailed high-resolution STM studies of connectivity and branching exist.

Herein, we demonstrate the formation of two-component polymeric nanostructures on a Au(111) surface under UHV conditions. The branched surface polymer, which contains pores about 3–10 nm in dimension, is characterized by high-resolution STM and it is shown that its connectivity can be controlled by varying the kinetic parameters of the preparation procedure.

Figure 1a shows the investigated condensation polymerization reaction between an aromatic trisalicylaldehyde[14,15] (trialdehyde) and 1,6-diaminohexane (diamine), which results

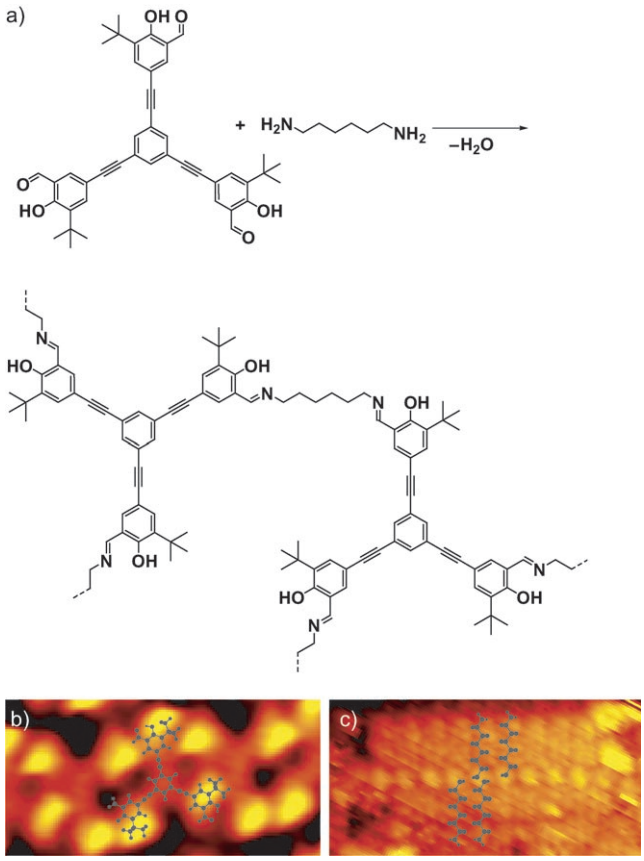

Figure 1. a) Condensation polymerization of a trialdehyde and 1,6-diaminohexane. STM images (60×30 Å^2) of b) a close-packed island of trialdehydes[14] (I_t = 0.60 nA, V_t = 1.05 V) and c) the lamellar structure of 1,6-diaminohexanes (I_t = 0.34 nA, V_t = −1.9 V). Molecular models are superimposed. I_t = tunneling current, V_t = tunneling voltage.

in a polymer connected by imine bonds. In solution the trialdehyde is known to form a cross-linked polymer by reaction with ethylenediamine.[15] Covalent interlinking of similar two-spoke salicylaldehydes and octylamine on Au(111) under UHV conditions was recently demonstrated by STM and synchrotron-based X-ray spectroscopy.[16]

STM images of the reactants adsorbed individually on the Au(111)-$(22\times\sqrt{3})$ surface are shown in Figure 1b and c. Upon co-deposition followed by annealing above 400 K, open filamentous structures are formed (Figure 2a). The local bonding pattern is revealed from high-resolution STM images

[*] M. M. Knudsen, Prof. K. V. Gothelf
Danish National Research Foundation
Centre for DNA Nanotechnology at iNANO and Department of Chemistry
University of Aarhus
Langelandsgade 140, 8000 Aarhus C (Denmark)
E-mail: kvg@chem.au.dk
Dr. S. Weigelt, Dr. C. Busse, Dr. C. Bombis, Assoc. Prof. E. Lægsgaard, Prof. F. Besenbacher, Assoc. Prof. T. R. Linderoth
Interdisciplinary Nanoscience Center (iNANO) and Department of Physics and Astronomy
University of Aarhus
Ny Munkegade, 8000 Aarhus C (Denmark)
Fax: (+45) 8942-3690
E-mail: trolle@phys.au.dk

Supporting information for this article is available on the WWW under http://www.angewandte.org or from the author.

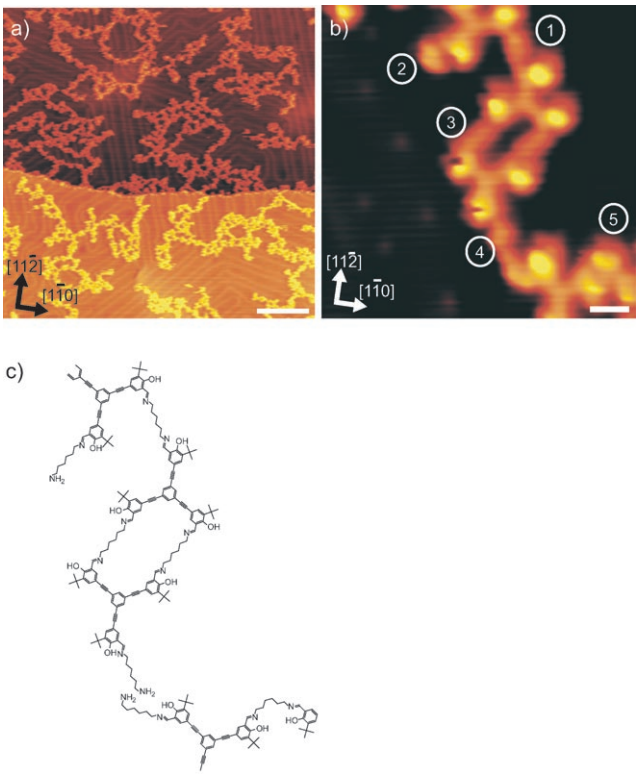

Figure 2. On-surface condensation polymerization. a) Large-scale STM image ($V_t = -1.4$ V, $I_t = -0.66$ nA; scale bar: 200 Å). b) High-resolution STM image revealing the local bonding pattern. The numbers refer to bonding geometries discussed in the text ($V_t = 1.5$ V, $I_t = 0.34$ nA; scale bar: 10 Å). c) Model of the structure in (b).

(Figure 2b). The trialdehydes can be identified from their characteristic Y shape with protrusions originating from the *tert*-butyl groups. The trialdehydes are linked together by rodlike features attributed to the alkyl chains of the diamines. The alkyl chains always extend from the side of the spoke opposite to the bright *tert*-butyl group, as expected for the imine reaction product (see Figure 1a). This STM signature is similar to that found for the monomeric reaction product formed under similar conditions,[16] and we therefore attribute all interlinks between trialdehydes and alkyl chains to covalent imine bonds.

All spokes of the trialdehydes are saturated by reaction with diamines. Two trialdehydes can be covalently connected either through one alkyl chain (1 and 5 in Figure 2b), or by two chains in a characteristic double-bonded motif (3 in Figure 2b). The alkyl linkers can be straight, as in bonding geometries 1 and 3, but are also often imaged with a compressed/bent shape (5 in Figure 2b), which we tentatively attribute to *gauche* defects in the chain. Alkyl chains connected to a trialdehyde at only one end are also observed (2 and 4 in Figure 2b). When the chain is free at the other end, it is imaged as a smeared-out feature (2), which is attributed to rapid thermal motion. If two such unbound ends meet, they pair head-to-head, which is observed as rodlike features (4) with twice the length of a single diamine. We propose that hydrogen bonding between the free amino groups occurs at these positions.

To investigate if order and connectivity in the polymer can be controlled, two different preparation procedures were applied. In both cases trialdehyde was first dosed onto the surface. In method A, the sample was subsequently exposed to 1,6-diaminohexane ($p = 1\text{–}5 \times 10^{-7}$ mbar) at 120–160 K leading to the formation of multilayers. Reaction was induced by annealing at 400–450 K. In method B, the sample with adsorbed trialdehyde was heated to 400 K and exposed to a lower pressure (5×10^{-9} mbar) of 1,6-diaminohexane. Characteristic structures resulting from methods A and B are shown in Figure 3a and b, respectively. In the corresponding

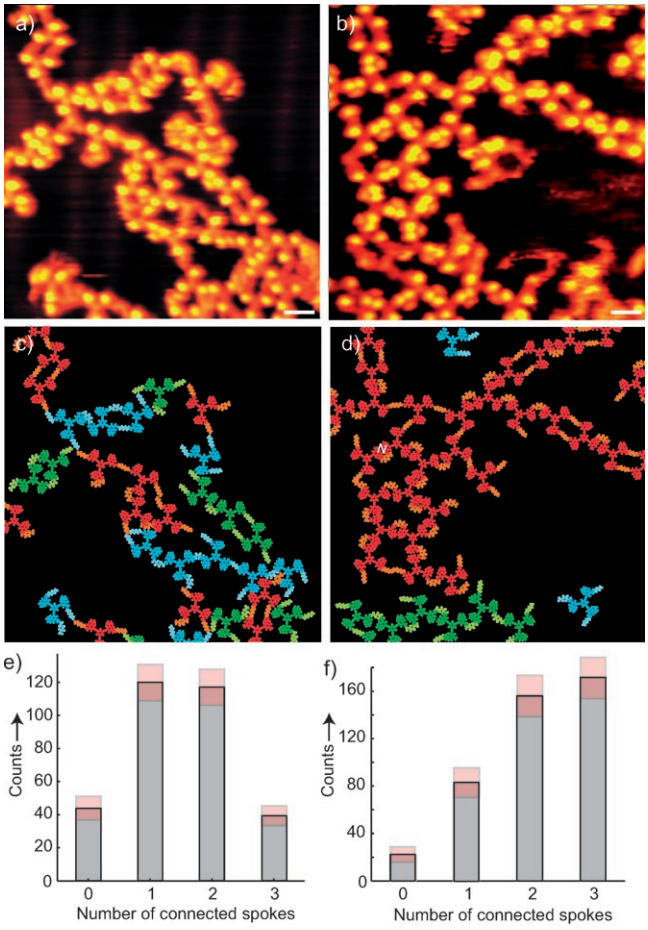

Figure 3. Covalent connectivity. a,b) STM images obtained after preparation methods A and B ($V_t = 1.5$ V, $I_t = 0.35$ nA/$V_t = -1.4$ V, $I_t = 0.27$ nA, respectively; scale bars: 20 Å). c,d) Models of the structures in (a) and (b) showing individual oligomers/polymers in different colors. e,f) Histograms showing the occurrence of trialdehydes with 0–3 spokes covalently connected to another trialdehyde after preparation methods A and B, respectively. The pink boxes indicate one standard deviation. Each histogram is based on STM data obtained in three independent experiments. No significant differences were observed for experiments with the same preparation method.

models (Figure 3c,d) each macromolecule formed by a continuous series of covalent imine interlinkages has been color coded individually.

Preparation method A favors the formation of smaller oligomers, whereas extended polymers result from method B

(the largest polymers extend out of the STM images acquired with submolecular resolution and contain over 50 trialdehydes). The histograms of Figure 3e and f show the occurrence of trialdehydes with 0–3 molecular spokes covalently linked through a single alkyl chain to neighboring trialdehydes, which reveals a significantly higher degree of connectivity with method B. From the histograms we find the probability P for a given spoke to be covalently connected to a spoke of a neighboring trialdehyde to be $P_A = 0.49 \pm 0.03$ and $P_B = 0.70 \pm 0.03$ for preparation methods A and B, respectively. The connectivity P_B is well above the Flory–Stockmayer[17] critical value ($P_c = 0.5$), which implies that the formation of infinite polymeric networks on the surface should be achievable at sufficiently high coverage.

The distinct difference in connectivity resulting from the two preparation procedures is primarily attributed to kinetic conditions during the reaction. In method A, ordered islands of trialdehydes are covered by multilayers of diamine. Upon heating to the temperature necessary for reaction, the ready availability of diamines leads to a high probability of saturating each trialdehyde spoke with a diamine, which results in a low connectivity in the structure. In method B, the amines are supplied at a higher substrate temperature where the trialdehyde islands are partially dissolved and there are free diffusing trialdehydes.[15] The temperature is above the amine desorption temperature, but a low surface concentration of amines is maintained by adsorption–desorption equilibrium. Compared to method A, trialdehydes with one or more alkyl amines attached are therefore more likely to encounter and react with unreacted trialdehyde spokes before these are saturated by free diamines, thus leading to an increased connectivity. Additional factors influencing the ordering are conformational flexibility of the trialdehydes[14] and a possible reversibility of imine formation in the presence of free amines that should be able to attack and replace existing imine bonds.

The highly connected polymer prepared by method B displays both 2D networks and 1D wires. The wires (Figure 4b) are composed of double-bonded trialdehydes (compare with 3 in Figure 2b) which have their remaining spokes connected to adjacent dimers. Sometimes the ends of a wire react resulting in ring closure (Figure 4b, top right). In the networks (Figure 4a), the trialdehydes constitute branching points with each trialdehyde connected to three neighbors. The interlinking alkyl chains are typically bent. Areas with network structure are more abundant than areas with chain formation. This finding is quantified by the proportion of trialdehydes forming branching points (26%) compared to trialdehydes acting as nonterminating chain segments (13%). The remaining trialdehydes (60%) contain at least one noninterlinked spoke.

Pores can be found in the networks with diameters from about 3 to 10 nm (Figure 5a–f). The abundance of pores formed from up to eight trialdehydes is plotted in Figure 5h.

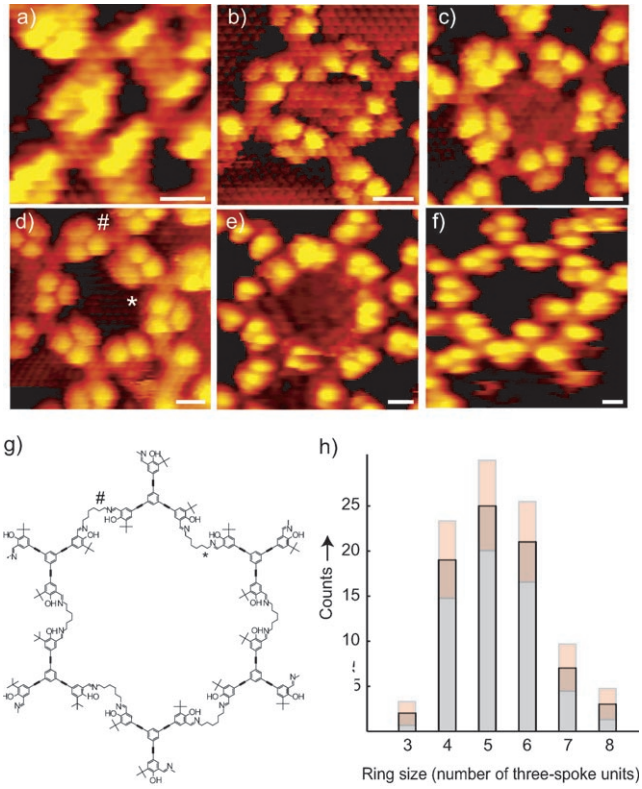

Figure 5. Network pores. STM images of pores involving a) three, b) four, c) five, d) six, e) seven, and f) eight trialdehydes (scale bar: 1 nm). g) The six-membered pore in (d) with alkyl linkers placed at the inner (*) and outer (#) pore wall. h) Distribution of observed pore sizes. Pink boxes indicate one standard deviation.

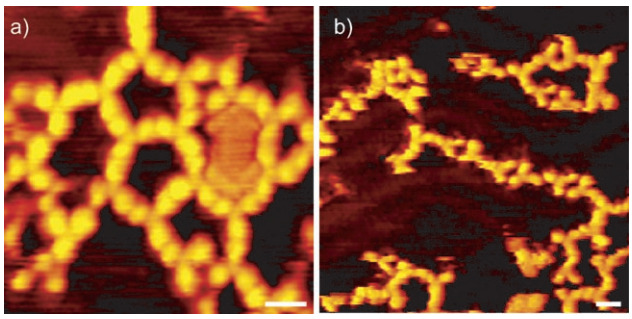

Figure 4. Network and chain-type polymeric structures. STM images of a domain with a) network formation ($V_t = -2.0$ V, $I_t = 0.31$ nA; scale bar: 20 Å) and b) chain formation ($V_t = -2.0$ V, $I_t = 0.33$ nA; scale bar: 20 Å). The images were obtained in an STM mode where only the aromatic system of the trialdehydes is visualized clearly.[14]

A preference for rings with four to six interlinked trialdehydes is found. The ring-size selection is speculated to result from 1) kinetic competition between the process of adding further trialdehydes and intramolecular ring closure, which disfavors large pore sizes, and 2) thermodynamic favoring of structures with optimized bonding angles, which may explain the low abundance of three-membered rings.

The detailed bonding pattern in the pores provides support for the notion that bending strain in the alkyl chains affects pore formation. The drawing in Figure 5g of the six-membered pore in Figure 5d illustrates that the interlinking alkyl chains can be positioned at either the inner or the outer pore wall (* and # in Figure 5g,

respectively). The distribution over these two positions as a function of pore size is shown in Table 1. In a six-membered pore, all pairwise interlinked trialdehyde spokes can be parallel (Figure 5g), whereas the internal angle between interlinked spokes should be concave (convex) for the smaller (larger) pores. A concave (convex) angle can be realized by placing the linker on the outside (inside) of the pore, as this leads to the least bending in the alkyl chain. Thus, four- and five-membered pores minimize the strain by placing the alkyl chains on the outside. The six-membered pores are nearly free of bending and the position is arbitrary. The seven-membered pores exhibit a marginal tendency to place the alkyl chains on the inside.

Table 1: Position of interlinking alkyl chains in pores with different numbers of trialdehydes.

Pore size	Four-ring	Five-ring	Six-ring	Seven-ring
Outside (#)	72	52	39	8
Inside (*)	4	33	33	13

In summary, we have formed covalently interlinked 2D polymers on a Au(111) surface which locally exhibit domains with nanometer-sized pores. The polymer connectivity is controlled by kinetic parameters during the synthesis on the surface. Covalently interlinked surface nanostructures are expected to exhibit interesting collective electronic properties and to have a higher thermal and chemical stability compared to structures formed by conventional surface self-assembly. Porous molecular networks are promising templates, for example, for host–guest sensing applications.[18] Further studies aim to improve the long-range order of the investigated 2D surface polymers.

Experimental Section

The experiments were performed in a UHV system equipped with a variable-temperature Aarhus scanning tunneling microscope[19] (see also http://www.specs.de). The herringbone reconstructed Au(111) $(22 \times \sqrt{3})$ surface was prepared by argon-ion sputtering at 1.5 kV and annealing to 850 K. The trialdehyde (1,3,5-tris[(5-*tert*-butyl-3-formyl-4-hydroxyphenyl)ethynyl]benzene)[15] was vapor-deposited onto the substrate from a heated glass crucible. The 1,6-diaminohexane (> 99%, Fluka) was dosed from a glass vial onto the substrate through a leak valve in an isolated reaction cell.

In both preparation methods a subsaturation coverage of trialdehydes (less than a third of a monolayer as estimated by STM) was formed by deposition on a sample held at about 300 K. In method A the sample was saturated with 1,6-diaminohexane by dosing for 1–2 min at a background pressure of $1–5 \times 10^{-7}$ mbar while the sample was held at 120–160 K. Upon heating to room temperature, imine oligomers embedded in a matrix of diamines were observed (see the Supporting Information, Figure S1). Further heating to 450 K resulted in desorption of unreacted diamines. In method B the sample with adsorbed trialdehydes was heated to 400 K and exposed to a low pressure (5×10^{-9} mbar) of 1,6-diaminohexane for about 30 min at this temperature. After exposure the sample was flashed to 400 K in the main chamber. STM imaging was performed at temperatures in the range of 120–160 K.

Received: November 2, 2007
Revised: January 18, 2008
Published online: April 29, 2008

Keywords: nanostructures · polymerization · polymers · scanning probe microscopy · self-assembly

[1] a) S. De Feyter, F. C. De Schryver, *Chem. Soc. Rev.* **2003**, *32*, 139; b) J. V. Barth, *Annu. Rev. Phys. Chem.* **2007**, *58*, 375.
[2] a) K. W. Hipps, L. Scudiero, D. E. Barlow, M. P. Cooke, *J. Am. Chem. Soc.* **2002**, *124*, 2126; b) M. Schöck, R. Otero, S. Stojkovic, F. Hummelink, A. Gourdon, E. Lægsgaard, I. Stensgaard, C. Joachim, F. Besenbacher, *J. Phys. Chem. B* **2006**, *110*, 12835; c) S. Berner, M. Brunner, L. Ramoino, H. Suzuki, H. J. Güntherodt, T. A. Jung, *Chem. Phys. Lett.* **2001**, *348*, 175.
[3] a) T. Yokoyama, S. Yokoyama, T. Kamikado, Y. Okuno, S. Mashiko, *Nature* **2001**, *413*, 619; b) S. Berner, M. de Wild, L. Ramoino, S. Ivan, A. Baratoff, H. J. Güntherodt, H. Suzuki, D. Schlettwein, T. A. Jung, *Phys. Rev. B* **2003**, *68*.
[4] a) J. A. Theobald, N. S. Oxtoby, M. A. Phillips, N. R. Champness, P. H. Beton, *Nature* **2003**, *424*, 1029; b) M. Stöhr, M. Wahl, C. H. Galka, T. Riehm, T. A. Jung, L. H. Gade, *Angew. Chem.* **2005**, *117*, 7560; *Angew. Chem. Int. Ed.* **2005**, *44*, 7394; c) G. Pawin, K. L. Wong, K. Y. Kwon, L. Bartels, *Science* **2006**, *313*, 961.
[5] a) N. Lin, A. Dmitriev, J. Weckesser, J. V. Barth, K. Kern, *Angew. Chem.* **2002**, *114*, 4973; *Angew. Chem. Int. Ed.* **2002**, *41*, 4779; b) A. Dmitriev, H. Spillmann, N. Lin, J. V. Barth, K. Kern, *Angew. Chem.* **2003**, *115*, 2774; *Angew. Chem. Int. Ed.* **2003**, *42*, 2670.
[6] L. Grill, M. Dyer, L. Lafferentz, M. Persson, M. V. Peters, S. Hecht, *Nat. Nanotechnol.* **2007**, *2*, 687.
[7] S. F. Alvarado, W. Riess, M. Jandke, P. Strohriegl, *Org. Electron.* **2001**, *2*, 75.
[8] a) P. C. M. Grim, S. De Feyter, A. Gesquiere, P. Vanoppen, M. Rucker, S. Valiyaveettil, G. Moessner, K. Mullen, F. C. De Schryver, *Angew. Chem.* **1997**, *109*, 2713; *Angew. Chem. Int. Ed. Engl.* **1997**, *36*, 2601; b) Y. Okawa, M. Aono, *Nature* **2001**, *409*, 683; c) O. Endo, H. Ootsubo, N. Toda, M. Suhara, H. Ozaki, Y. Mazaki, *J. Am. Chem. Soc.* **2004**, *126*, 9894.
[9] a) K. Sugiura, H. Tanaka, T. Matsumoto, T. Kawai, Y. Sakata, *Chem. Lett.* **1999**, 1193; b) H. Kasai, H. Tanaka, S. Okada, H. Oikawa, T. Kawai, H. Nakanishi, *Chem. Lett.* **2002**, 696; c) O. Shoji, H. Tanaka, T. Kawai, Y. Kobuke, *J. Am. Chem. Soc.* **2005**, *127*, 8598.
[10] N. Bampos, C. N. Woodburn, M. E. Welland, J. K. M. Sanders, *Angew. Chem.* **1999**, *111*, 2949; *Angew. Chem. Int. Ed.* **1999**, *38*, 2780.
[11] a) H. Sakaguchi, H. Matsumura, H. Gong, *Nat. Mater.* **2004**, *3*, 551; b) H. Sakaguchi, H. Matsumura, H. Gong, A. M. Abouelwafa, *Science* **2005**, *310*, 1002.
[12] a) P. Samorí, V. Francke, K. Müllen, J. P. Rabe, *Chem. Eur. J.* **1999**, *5*, 2312; b) E. Mena-Osteritz, A. Meyer, B. M. W. Langeveld-Voss, R. A. J. Janssen, E. W. Meijer, P. Bäuerle, *Angew. Chem.* **2000**, *112*, 2791; *Angew. Chem. Int. Ed.* **2000**, *39*, 2679; c) M. Brun, R. Demadrille, P. Rannou, A. Pron, J. P. Travers, B. Grevin, *Adv. Mater.* **2004**, *16*, 2087; d) L. Scifo, M. Dubois, M. Brun, P. Rannou, S. Latil, A. Rubio, B. Grevin, *Nano Lett.* **2006**, *6*, 1711.
[13] a) J. M. Bonello, R. M. Lambert, N. Kunzle, A. Baiker, *J. Am. Chem. Soc.* **2000**, *122*, 9864; b) S. Lavoie, M.-A. Laliberté, G. Mahieu, V. Demers-Carpentier, P. McBreen, *J. Am. Chem. Soc.* **2007**, *129*, 11668.

[14] a) C. Busse, S. Weigelt, L. Petersen, E. Lægsgaard, F. Besenbacher, T. R. Linderoth, A. H. Thomsen, M. Nielsen, K. V. Gothelf, *J. Phys. Chem. B* **2007**, *111*, 5850; b) S. Weigelt, C. Busse, L. Petersen, E. Rauls, B. Hammer, K. V. Gothelf, F. Besenbacher, T. R. Linderoth, *Nat. Mater.* **2006**, *5*, 112.
[15] M. Nielsen, A. H. Thomsen, T. R. Jensen, G. J. Jakobsen, J. Skibsted, K. V. Gothelf, *Eur. J. Org. Chem.* **2005**, 342.
[16] S. Weigelt, C. Busse, C. Bombis, M. M. Knudsen, K. V. Gothelf, T. Strunskus, C. Wöll, M. Dahlbom, B. Hammer, E. Lægsgaard, F. Besenbacher, T. R. Linderoth, *Angew. Chem.* **2007**, *119*, 9387; *Angew. Chem. Int. Ed.* **2007**, *46*, 9227.
[17] a) P. J. Flory, *J. Am. Chem. Soc.* **1941**, *63*, 3083; b) W. H. Stockmayer, *J. Chem. Phys.* **1943**, *11*, 45.
[18] a) S. Stepanow, M. Lingenfelder, A. Dmitriev, H. Spillmann, E. Delvigne, N. Lin, X. B. Deng, C. Z. Cai, J. V. Barth, K. Kern, *Nat. Mater.* **2004**, *3*, 229; b) S. J. H. Griessl, M. Lackinger, F. Jamitzky, T. Markert, M. Hietschold, W. M. Heckl, *Langmuir* **2004**, *20*, 9403; c) M. Stöhr, M. Wahl, H. Spillmann, L. H. Gade, T. A. Jung, *Small* **2007**, *3*, 1336.
[19] E. Lægsgaard, F. Besenbacher, K. Mortensen, I. Stensgaard, *J. Microsc.* **1988**, *152*, 663.

